

Mono-to-multilayer transition in growing bacterial colonies

Zhihong You,¹ Daniel J. G. Pearce,¹ Anupam Sengupta,² and Luca Giomi^{1,*}

¹*Instituut-Lorentz, Universiteit Leiden, P.O. Box 9506, 2300 RA Leiden, The Netherlands*

²*Physics and Materials Science Research Unit, University of Luxembourg,
162 A, Avenue de la Faencerie, L-1511 Luxembourg City, Luxembourg*

The transition from monolayers to multilayered structures in bacterial colonies is a fundamental step in biofilm development. Observed across different morphotypes and species, this transition is triggered within freely growing bacterial microcolonies comprising a few hundred cells. Using a combination of numerical simulations and analytical modeling, here we demonstrate that this transition originates from the competition between growth-induced in-plane active stresses and vertical restoring forces, due to the cell-substrate interactions. Using a simple chain-like colony of laterally confined cells, we show that the transition is triggered by the mechanical instability of individual cells, thus it is localized and mechanically deterministic. Asynchronous cell division renders the process stochastic, so that all the critical parameters that control the onset of the transition are continuously distributed random variables. Upon modeling cell division as a Poisson process, we can approximately calculate the probability distribution function of the position and time associated with the first extrusion. The rate of such a Poisson process can be identified as the order parameter of the transition, thus highlighting its mixed deterministic/stochastic nature.

The ability of forming biofilms is a robust and widely observed property across different bacterial species [1]. Despite the extraordinary diversity within prokaryotic microorganisms, nearly all bacteria, either as single species or in a community, possess the necessary biomolecular “toolkit” to colonize a range of natural or synthetic surfaces through autonomous production of extracellular matrix (ECM) [2]. For planktonic species (i.e., freely swimming), the life of a biofilm starts with cells undergoing a phenotypic shift whereby motile cells turn sessile (i.e. surface-associated), and thereafter continues growing in size via the formation of an exponentially growing monolayer of tightly packed and partially aligned cells [3–12]. Colonies originating from a single bacterium initially develop as a flat monolayer and, upon reaching a critical population, invade the third dimension forming multiple layers [13–16].

Such a transition from mono to multilayered structure has recently drawn significant attention in the biophysical literature, being a universal step in biofilm formation, as well as a process where mechanical forces are likely to play a leading role. Grant *et al.* [14] explored the effect of substrate elasticity in *E. coli* colonies confined between glass and agarose and found that this affects the size of the colony at the onset. In this respect, the mono-to-multilayer transition shares some similarity with the buckling instability of an elastic plate subject to lateral pressure (see e.g. Ref. [17]). More recently, Beroz *et al.* [16] demonstrated that, in *V. cholerae* biofilms, escape to the third dimension is mediated by a *verticalization* of the longer cells. Similar mechanisms are also found in confluent monolayers of eukaryotic cells [18–27] and are believed to regulate cell extrusion and apoptosis.

These works have greatly contributed to shed light on the problem, however, a general understanding of

the physical mechanisms underpinning the mono-to-multilayer transition is still lacking, with questions far outnumbering the answers so far: 1) Does the instability result from collective or local effects? 2) Is there a well defined critical size, stress, and time at which extrusion is first triggered? 3) To what extent do the mechanical properties of the cells and the substrate mediate extrusion? 4) Is the mono-to-multilayer transition a deterministic process, or does it result from an interplay of deterministic and stochastic effects?

In this Letter we address these questions theoretically, using a combination of numerical and analytical methods. We demonstrate that the mono-to-multilayer transition in a system of growing rod-like cells results from a competition between the in-plane active stresses, that compress the cells laterally, and the vertical restoring forces, owing to the cell-substrate interactions (e.g. cell-substrate adhesion). As the colony expands the internal stress increases until it is sufficiently large to cause extrusion of the first cells. In the ideal case of a chain-like colony of compressed laterally-confined non-growing cells, the transition is entirely deterministic and the critical stress at which extrusion initiates can be calculated analytically. Asynchronous cell division, however, renders the transition stochastic. In this case, the critical stress is a continuously distributed random variable and the first extrusion does not necessarily occur at the colony center, despite this being the region of maximal stress. Upon modeling cell division as a Poisson process, we can approximately calculate the probability distribution function (PDF) of the position and time associated with the first extrusion. Finally, we show that rate of the Poisson process, is analogous to an order parameter and that, in this respect, the mono-to-multilayer instability is likened

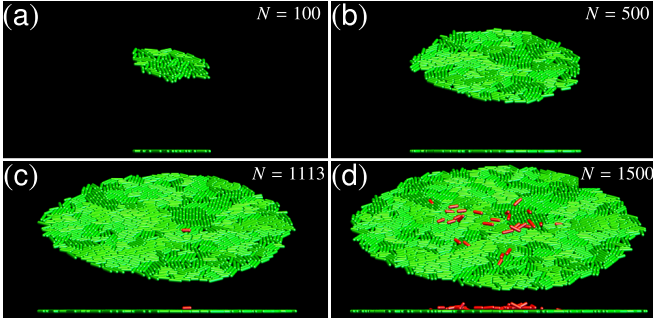


FIG. 1. Snapshots of a simulated growing colony at different ages to show the mono-to-multilayer transition. The lower image in each panel shows the side view. In panels (c) and (d), the extruded cells are highlighted as red.

to a continuous phase transition.

We employ a minimal model of duplicating bacteria, where cells are represented as spherocylinders with a fixed diameter d_0 and a time-dependent length l (excluding the caps on both ends), growing in three-dimensional space [11, 28]. Whereas cells in bacterial colonies are potentially subject to a large variety of mechanical and biochemical stimuli, here we focus on three types of force: the repulsive forces associated with cell-cell and cell-substrate steric interactions and a vertical restoring force, representing either the attractive force due to adhesion of the cells with the ECM [16], or a mechanical compression from above [14, 15]. All forces are treated as Hookean and, for simplicity, we set the elastic constant of the repulsive forces to be the same, k , and that of the attractive force to $k_a l$, to mimic the dependence of the restoring forces on the contact area. The length l_i of the i -th cell increases in time with rate g_i and, after having reached the value l_d , the cell divides into two identical daughter cells. To avoid synchronous divisions, the growth rate of each cell is randomly chosen in the interval $g/2 \leq g_i \leq 3g/2$, with g the average growth rate. More detail about the model can be found in Ref. [29]. Fig. 1 shows typical configurations of our *in silico* colonies at different time points. Consistent with the experimental evidence [13, 14], the colony initially expands as a perfect monolayer (Figs. 1a,b) and, once it is sufficiently large, some cells are extruded and originate a second layer (Figs. 1c,d). See Ref. [29] for time-lapse animations showing the growth dynamics of the colonies.

As a starting point, we look at a simplified chain-like colony, consisting of a row of cells confined in a channel (Fig. 2a). The cells have identical length l and do not grow, but are compressed by a pair of forces f applied at the two ends of the channel. As in the case of disk-like colonies (Fig. 1), cells remain attached to the substrate for small compressive forces and are extruded to the second layer for large f values. In this case, the transition is entirely deterministic and there exists a

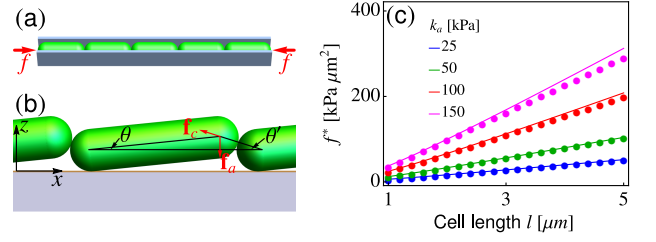


FIG. 2. (a) Schematic diagram of the chain-like colony. (b) Schematics of torque balance about the lower end of the cell. (c) Critical force as a function of the cell length, for various k_a values. The dots and lines represent respectively the simulation and analytical results as in Eq. 1.

well defined critical force, f^* , at which the monolayer becomes unstable. This can be calculated analytically upon balancing the torques associated with cell-cell and cell-substrate interactions, about the lower end of the cell axis. Calling $\mathbf{p} = (\cos \theta, 0, \sin \theta)$ the orientation of the first extruded cell and $\mathbf{f}_c = f_c(-\cos \theta', 0, \sin \theta')$, with $f_c = f/\cos \theta'$, the contact force exerted by the nearby cell (Fig. 2b), the lifting torque can be calculated in the form: $\tau_c = l(p_x f_z - p_z f_x) = l f \cos \theta (\tan \theta + \tan \theta')$. Analogously, the restoring torque resulting from the adhesive force is $\tau_a = k_a l^3 \sin \theta \cos \theta$. In a perfectly horizontal monolayer, $\theta = \theta_0 = 0$ and both torques vanish. In order for such a configuration to be stable against slight orientational fluctuations of magnitude $\delta \theta \ll 1$, $\tau_c(\theta_0 + \delta \theta) < \tau_a(\theta_0 + \delta \theta)$. Upon expanding τ_c and τ_a at the linear order in $\delta \theta$ and approximating $\theta' \approx (l/d_0)\theta$, one can verify that such a stability condition breaks down when $f > f^*$, with:

$$f^* = k_a l^2 \left(1 + \frac{l}{d_0}\right)^{-1}, \quad (1)$$

in excellent agreement with the result of our numerical simulations (Fig. 2c). The existence of a well defined critical force resulting from the competition between compression and rotation is vaguely reminiscent of Euler's buckling in elastic rods. However, while buckling is a system-wide instability, the mono-to-multilayer transition is determined by torque balance at the length scale of a single cell.

Next we explore the effect of asynchronous cell division. Cells are again confined in the channel and, unlike the previous case, they are not subject to lateral compression, but elongate and divide. To investigate the effect of the key parameters, k_a , l_d , and g , we perform four sets of 10^5 simulations, starting from a single cell at the equilibrium configuration. In the “control” set, we fix $k_a = 50$ kPa, $l_d = 4$ μm , and $g = 2$ $\mu\text{m}/\text{h}$. In each of the remaining three sets we change one of the parameters.

As the colony expands, the longitudinal stress (calculated via the virial construction [29]) progressively builds

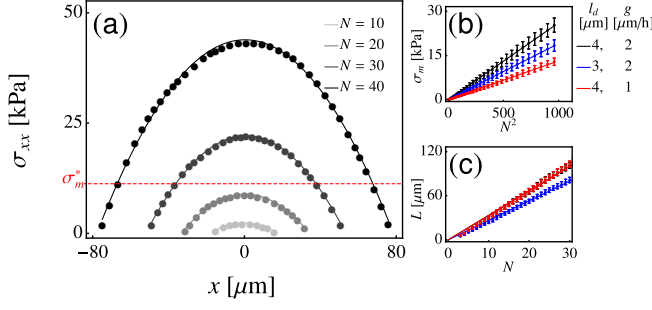


FIG. 3. (a) The spatial distributions of stress in growing chain-like colonies at different ages, at the control parameters. (b) Maximum stress σ_m and (c) colony length L as a function of cell number N , for different sets of parameters. The error bars show the standard deviation of results from 10000 runs about the average values. Solid lines indicate the best fit, linear or parabolic, to the data points.

up, while preserving a simple parabolic profile of the form:

$$\sigma_{xx}(x) = \sigma_m \left[1 - \left(\frac{2x}{L} \right)^2 \right], \quad (2)$$

where σ_m and L represent respectively the maximum stress and the colony length (Fig. 3a). Numerically, we find that $\sigma_m = aN^2$ and $L = bN$ (Fig. 3b,c), where N is the total number of cells and a and b are constants depending only on the division length l_d and the growth rate g . Because the stress is maximal at the center of the colony, one would expect the first extrusion to occur here. Our simulations, however, show a dramatically different behavior. Specifically, the position of the first extruded cell x^* follows a broad distribution, whose spread is comparable to the size of the colony itself (Fig. 4a). Analogously the transition time t^* (Fig. 4b) and the critical stress σ^* experienced by cells at the verge of extrusion (Fig. 4c), are continuously distributed random variables.

The lack of well defined critical stress is in stark contrast with the classical buckling scenario, but shares some similarity with the onset of fracture in heterogeneous media [30]. In the following, we demonstrate that, in growing bacterial colonies, this behavior results from the combined inherent randomness of the division process and the local nature of the instability. According to Eq. (1) a cell is unstable to extrusion if subject to a critical force whose magnitude increases with the cell length. In a growing colony, a division event introduces a sudden drop in the cell length and this can, in turn, trigger an extrusion instability, as long as the cell is subject to a stress larger than that required to extrude a cell of minimal length $l_m = (l_d - d_0)/2$. A similar phenomenon was found in [16]. We denote such a minimal critical stress σ_m^* . As the stress is spatially inhomogeneous and increasing in time, there will be a whole region, symmetric with respect to

the center of the colony and whose length increases in time, where the local stress exceeds σ_m^* and cell division can trigger the first extrusion. We call this region the P-zone. The probability associated with the first extrusion is then equal to the probability of having a division within the P-zone. This can be calculated as follows.

Let us consider a colony of n cells with growth rate g and assume that, at an arbitrary time, their lengths are independent and uniformly distributed in the interval $l_m \leq l \leq l_d$. After a time t , the probability that no division has yet occurred equates the probability that none of the cells is initially longer than $l_d - gt$:

$$P(t) = \left(\frac{l_d - gt - l_m}{l_d - l_m} \right)^n \approx e^{-\lambda(n)t}, \quad (3)$$

where $\lambda(n) = ng/(l_d - l_m)$ and the approximation holds for large n values. Eq. (3) defines a Poisson process of rate $\lambda(n)$ [31]. If n is time-dependent, the process becomes inhomogeneous, but the probability preserves the same structure, with $\lambda(t) = \lambda[n(t)]$ and $P(t) = e^{-\int_0^t dt' \lambda(t')}$ [31]. The PDF associated with observing the first division at time t is then:

$$f(t) = \frac{d}{dt}[1 - P(t)] = \lambda(t)e^{-\int_0^t dt' \lambda(t')}. \quad (4)$$

In our case, n represents the number of cells within the P-zone. This is, on average, $n = L^*/\bar{l}$, where L^* is the length of the P-zone and $\bar{l} = (l_d + l_m)/2$ the average cell length. L^* can be calculated by solving $\sigma_{xx}(L^*/2) = \sigma_m^*$ (red dashed line in Fig. 3a). This yields: $L^* = b\sqrt{N^2(t) - N_0^2}$, with $N_0 = \sqrt{\sigma_m^*/a}$ is the minimal number of cells required for the P-zone to exist. From this and Eq. (3), we can calculate the rate $\lambda(t)$ as:

$$\lambda(t) = \frac{2gb}{l_d^2 - l_m^2} \sqrt{N^2(t) - N_0^2} \sim [N(t) - N_0]^{1/2}. \quad (5)$$

Eq. (5) highlights the role of λ as order parameter for the mono-to-multilayer transition. For $N(t) < N_0$, λ is imaginary and the probability of observing an extrusion vanishes identically. On the other hand, for $N(t) > N_0$, λ is real and the probability of observing an extrusion increases in time. The transition is continuous in this case, but other scenarios are likely possible.

To make the time-dependence explicit in Eq. (5), we need to calculate $N(t)$. Evidently, the average number of cells in the colony grows exponentially in time. Because cells have random growth rates, the time t taken for the colony to attain a given population size $N(t)$, is a random variable of the form $t = \bar{t} + \Delta t$ (Fig. S3 in Ref. [29]). Numerically, we find that Δt follows a Gaussian distribution, $\mathcal{N}(0, \delta_{\Delta t}^2)$, having zero mean and whose variance, $\delta_{\Delta t}^2$, depends on l_d and g [29]. Taking $N(t) = \exp[\omega(t - \Delta t)]$, with ω a constant, substituting it in Eq. (5) and integrating over Δt , yields the PDF

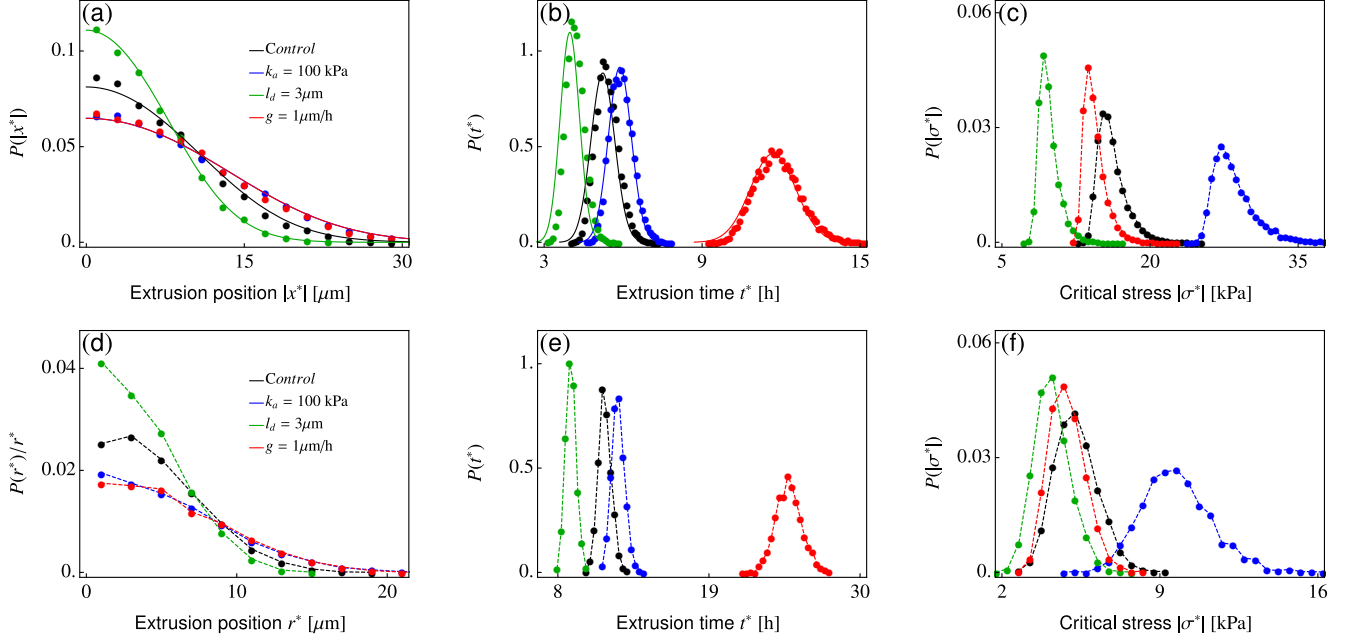


FIG. 4. (a-c) Probability densities of (a) the extrusion positions $|x^*|$, (b) the extrusion time t^* , and (c) the critical stress σ^* , for chain-like colonies of asynchronously dividing cells. (d) Probability density of the extrusion position r^* in disk-like colonies, normalized by r^* , the distance from the point of extrusion to the centroid of the colony. (e-f) Same as panels (b-c), but for disk-like colonies. More details about measuring these quantities can be found in [29]. In all panels, dots and dashed lines correspond to the simulation results and the solid lines to the analytical predictions. In each set of simulations, one parameter is changed compared to the control set, whose parameter values are indicated in the legends. The statistical results for each set of parameters are collected from 10000 runs for chain-like colonies, and 2000 runs for disk-like colonies.

associated with observing the first extrusion at time t^* :

$$p(t^*) = \int_{-\infty}^{t^*-t_0} d\Delta t \mathcal{N}(0, \delta_{\Delta t}^2) f(t^*|\Delta t), \quad (6)$$

with $f(t|\Delta t) = f[N(t)]$ the conditional PDF at fixed Δt and $t_0 = \omega^{-1} \log(N_0)$ the average time at which the P-zone first appears. The resulting probability distribution is displayed in Fig. 4b (solid lines) and is in excellent agreement with the numerical data. Similarly, we can calculate the probability distribution associated with the extrusion occurring at position x^* . From previous considerations, one can reasonably assume the extrusion location to be uniformly distributed within the P-zone. Thus the conditional PDF associated with observing the first extrusion at time t and position x is $f(x, t|\Delta t) = f(t|\Delta t)/L^*$, with $-L^*/2 \leq x \leq L^*/2$. Integrating over t and Δt yields:

$$p(x^*) = \int_0^\infty dt \int_{-\infty}^{t-t_0} d\Delta t \mathcal{N}(0, \delta_{\Delta t}^2) f(x^*, t|\Delta t), \quad (7)$$

again in excellent agreement with the numerical data (Fig. 4a). Further detail about the derivations can be found in [29]. Finally, Figs. 4d-e show the probability distributions of the extrusion position, extrusion time and critical stress for the original disk-like colonies (e.g.

Fig. 1). Despite the mechanical interactions being more complex in disk-like colonies [11, 29], the physical picture emerging from the simulations is nearly identical to that discussed for chain-like colonies.

The enormous variety of physical and biochemical mechanisms observed in cellular systems defeats the notion of universality, despite this, biofilms and tissues feature traits that are consistently found across several morphotypes and species, such as the capability of transitioning from simple monolayers to more complex multi-layered structures [14–16, 18–21]. Whereas this transition manifests itself in a multitude of possible variants, depending upon the nature of the environmental and intercellular forces, it robustly relies on a limited number of fundamental principles, which most cellular systems have in common. First, the interplay between steric interactions and active motion or growth, drives the formation of coherent structures on the plane, such as nematic domains [11], topological defects [21] or large groups of collectively moving cells [32]. Second, the extensile stresses arising from the in-plane spatial organization and the lack of vertical confinement, drives the cellular layer to be unstable to extrusion. Because intercellular forces are mainly repulsive, this process occurs at the scale of individual cells, in spite of the collective origin of the in-plane stresses driving the instability. Third, the transition is

both deterministic and stochastic. For a given configuration of the colony, there is well defined critical stress, related with the cells *local* arrangement (e.g. cell length and nematic order). But, as this is inherently random, so is the critical stress and, consequently, the extrusion time and position. Therefore, there is no uniquely defined critical state, but rather an ensemble of them. Upon modeling cell division as a Poisson process, and under the assumption that newly divided cells are the first to be extruded, we were able to reconstruct the probability distribution of the extrusion time and position for a simple laterally-confined chain-like colony, finding excellent agreement with our numerical data. The rate λ of the Poisson process is analogous to the order parameter in phase transitions and, as the transition depends on the details of the system uniquely via λ , we expect our result to be generic and carry over to other systems, as long as λ can be derived or approximated.

ZY, DJGP and LG are supported by The Netherlands Organization for Scientific Research (NWO/OCW) as part of the Frontiers of Nanoscience program and the Vidi scheme. AS was supported by the ATTRACT Investigator Grant of the Luxembourg National Research Fund (FNR).

* giomi@lorentz.leidenuniv.nl

- [1] J. W. Costerton, P. S. Stewart, and E. P. Greenberg, *Science* **284**, 1318 (1999).
- [2] D. McDougald, S. A. Rice, N. Barraud, P. D. Steinberg, and S. Kjelleberg, *Nat. Rev. Microbiol.* **10**, 39 (2012).
- [3] H. Cho, H. Jönsson, K. Campbell, P. Melke, J. W. Williams, B. Jedynak, A. M. Stevens, A. Groisman, and A. Levchenko, *PLoS Biol.* **5**, e302 (2007).
- [4] D. M. Morris and G. J. Jensen, *Ann. Rev. Biochem.* **77**, 583 (2008).
- [5] D. Volfson, S. Cookson, J. Hasty, and L. S. Tsimring, *Proc. Natl. Acad. Sci. U. S. A.* **105**, 15346 (2008).
- [6] D. Boyer, W. Mather, O. Mondragón-Palomino, S. Orozco-Fuentes, T. Danino, J. Hasty, and L. S. Tsimring, *Phys. Biol.* **8**, 026008 (2011).
- [7] S. Orozco-Fuentes and D. Boyer, *Phys. Rev. E* **88**, 012715 (2013).
- [8] T. J. Rudge, F. Federici, P. J. Steiner, A. Kan, and J. Haseloff, *ACS Synth. Biol.* **2**, 705 (2013).
- [9] A. Persat, C. D. Nadell, M. K. Kim, F. Ingremeau, A. Siryaporn, K. Drescher, N. S. Wingreen, B. L. Bassler, Z. Gitai, and H. A. Stone, *Cell* **161**, 988 (2015).
- [10] J. Sheats, B. Sclavi, M. C. Lagomarsino, P. Cicuta, and K. D. Dorfman, *R. Soc. Open Sci.* **4**, 170463 (2017).
- [11] Z. You, D. J.G. Pearce, A. Sengupta, and L. Giomi, *Phys. Rev. X* **8**, 031065 (2018).
- [12] D. Dell'Arciprete, M. L. Blow, A. T. Brown, F. D. C. Farrell, J. S. Lintuvuori, A. F. McVey, D. Marenduzzo, and W. C. K. Poon, *Nat. Commun.* **9**, 4190 (2018).
- [13] P.-T. Su, C.-T. Liao, J.-R. Roan, S.-H. Wang, A. Chiou, and W.-J. Syu, *PLoS ONE* **7**, e48098 (2012).
- [14] M. A. A. Grant, B. Waclaw, R. J. Allen, and P. Cicuta, *J. R. Soc. Interface* **11**, 20140400 (2014).
- [15] M. C. Duvernoy, T. Mora, M. Ardr, V. Croquette, D. Bensimon, C. Quilliet, J. M. Ghigo, M. Balland, C. Belloin, S. Lecuyer, N. Desprat, *Nat. Comm.* **1120 9**, (2018).
- [16] F. Beroz, J. Yan, Y. Meir, B. Sabass, H. A. Stone, B. L. Bassler, and N. S. Wingreen, *Nat. Phys.* **14**, 954 (2018).
- [17] S. P. Timoshenko, J. M. Gere, *Theory of elastic stability* (McGraw-Hill, New York, NY, 1961).
- [18] E. Marinari, A. Mehonic, S. Curran, J. Gale, T. Duke, and B. Baum, *Nature* **484**, 542 (2012).
- [19] R. Fernandez-Gonzalez, and J. A. Zallen, *Cell* **149**, 965 (2012).
- [20] L. Kocgozlu, T. Beng Saw, A. Phuong Le, I. Yow, M. Shagirov, E. Wong, R.-M. Mège, C. T. Lim, Y. Toyama, and B. Ladoux, *Curr. Biol.* **26**, 2942 (2016).
- [21] T. B. Saw, A. Doostmohammadi, V. Nier, L. Kocgozlu, S. Thampi, Y. Toyama, P. Marcq, C. T. Lim, J. M. Yeomans, and B. Ladoux, *Nature* **212**, 544 (2017).
- [22] G. T. Eisenhoffer, P. D. Loftus, M. Yoshigi, H. Otsuna, C.-B. Chien, P. A. Morcos, and J. Rosenblatt, *Nature* **484**, 546 (2012).
- [23] G. T. Eisenhoffer, and J. Rosenblatt, *Trends Cell Biol.* **23**, 185 (2013).
- [24] C. Guillot, and T. Lecuit, *Science* **340**, 1185 (2013).
- [25] G. M. Slatton and J. Rosenblatt, *Nat. Rev. Cancer* **14**, 495 (2014).
- [26] A. Ambrosini, M. Gracia, A. Proag, M. Rayer, B. Monier, and M. Suzanne, *Mech. Develop.* **144**, 33 (2017).
- [27] S. Ohsawa, J. Vaughn, and T. Igaki, *Dev. Cell* **44**, 284 (2018).
- [28] F. D. C. Farrell, O. Hallatschek, D. Marenduzzo, and B. Waclaw, *Mechanically Driven Growth of Quasi-Two-Dimensional Microbial Colonies*, *Phys. Rev. Lett.* **111**, 168101 (2013).
- [29] See supplementary information at <http://...>
- [30] M. J. Alava, P. K. V. V. Nukala, and S. Zapperi, *Adv. Phys.* **55**, 349 (2006).
- [31] J. F. C. Kingman, *Poisson Processes* (Clarendon Press, Oxford, 1992).
- [32] C. Blanch-Mercader, V. Yashunsky, S. Garcia, G. Duclos, L. Giomi, and P. Silberzan, *Phys. Rev. Lett.* **120**, 208101 (2006).